

Interference of Chirp Sequence Radars by OFDM Radars at 77 GHz

Christina Knill, Jonathan Bechter, and Christian Waldschmidt
Institute of Microwave Engineering, Ulm University, 89081 Ulm, Germany
Email: {firstname.lastname}@uni-ulm.de

Abstract—Radar sensors are common devices in daily traffic, especially for driver assistance and automotive safety systems. A high sensor density increases the probability of interferences, especially when the sensors occupy a large radar bandwidth. Many current sensors, e.g. chirp sequence radars, rely on frequency modulation schemes. A promising future radar concept applies orthogonal frequency division multiplexing (OFDM). This paper investigates the interference effect of an OFDM radar on a chirp sequence radar. Potential interference levels are derived and the influence of modulation parameters is evaluated with simulations.

I. INTRODUCTION

In the last few years, radar sensors became an important component of automotive safety and advanced driver assistance systems (ADAS). High resolution radar sensors are applied for environment perception and are key elements in future autonomous driving. It is expected that the amount of radar sensors operating in daily traffic will further increase significantly. Currently, most of those sensors rely on FMCW or chirp sequence modulation schemes.

In this context, the occurrence and the effects of interference of radar sensors have been investigated in the scientific community. In case of interference between two FMCW radars, time-limited spikes in the baseband signal is a common interference effect [1]. These interferences increase the overall noise floor in the receiver and can lead to sensor blindness. This effect is especially detrimental to the detection of targets like pedestrians or bicycles with a low radar cross section (RCS). However, it is very unlikely that ghost targets are generated by interferences [2], [3]. Similar interference effects can be shown for chirp sequence radars, cf. [4]. Multiple countermeasures already exist to this kind of interferences, like time domain signal repair [5], digital beamforming [6], [7], or frequency hopping [8].

New radar concepts focus on digitally generated multi-carrier wideband signals. A promising approach is orthogonal frequency division multiplexing (OFDM) [9]. The bandwidth occupied by an OFDM signal is split up into a large number of orthogonal equidistant subbands or subcarriers with maximum spectral density. All subcarriers are occupied simultaneously by a train of modulated transmit symbols on each subcarrier.

In Fig. 1 the transmit signals of a chirp and an OFDM radar operating in the same frequency range are shown. The OFDM signal and hence its transmit power is spread over

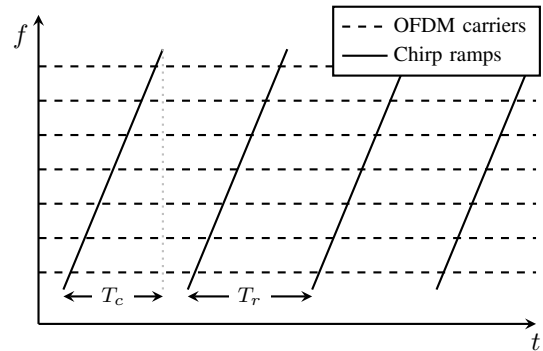


Fig. 1. Transmit signals of a chirp and an OFDM radar operating in the same frequency range; The chirp sequence radar transmits a series of linear frequency ramps (—) of duration T_c and with repetition time T_r . An OFDM radar transmits at the same time continuous waves at multiple carrier frequencies (---). For radar applications, hundreds of subcarriers are required.

a large bandwidth, therefore, we expect OFDM radars to cause interference. In this paper, these interference effects are investigated.

The paper is organized as follows. In Section II the signal models for the chirp sequence and OFDM radar are introduced and the interference signal and the power level in the chirp sequence receiver are derived. In Section III, the simulations are detailed and results are presented and evaluated.

II. SIGNAL MODELS AND RECEIVE POWER

To evaluate and investigate the influence of an interfering OFDM signal on a chirp sequence radar, mathematical models of both radar signals are required. The transmit and receive signals are described in the following.

A. Chirp Sequence Radar

The chirp sequence radar is modeled similarly to [10]. It transmits linear frequency ramps of the form

$$s_{Tx}(t) = \cos \left(2\pi \left(f_c t + \frac{B}{2T_c} t^2 \right) + \varphi_0 \right), \quad t \in [0, T_c], \quad (1)$$

with the carrier frequency f_c , chirp duration T_c , chirp bandwidth B , and an arbitrary phase φ_0 . The received signal reflected from a point target is the above signal time-shifted by the time of flight Δt :

$$s_{Rx}(t) \propto s_{Tx}(t - \Delta t). \quad (2)$$

At the receiver, the signal is down converted to the baseband by mixing with (1) and subsequently lowpass filtered. For a series of L transmitted frequency ramps (chirps), the following baseband signal is obtained for chirp $l = 0, \dots, L-1$ and a target at distance R :

$$s_{IF}(t) \propto \cos\left(2\pi\left(\frac{2f_c R}{c} + f_D T_r l + \left(\frac{2B R}{c T_c} + f_D\right)t\right)\right). \quad (3)$$

The time between two chirps is T_r , c the speed of light, and f_D describes the Doppler shift caused by the target's velocity. A steep ramp slope B/T_c is chosen, so that f_D is much smaller than $(2B R)/(c T_c)$. After applying a window function, the distance to the target is extracted by a Fourier transform along the time $t \in [0, T_c]$. The Doppler frequency is extracted by a Fourier transform along the chirp number l . These operations lead to a two-dimensional range-Doppler spectrum. Each target in the radar channel is represented by a peak in this spectrum.

B. OFDM Model

The OFDM signal is the interfering signal and will be denoted by the index I . An OFDM signal is composed of multiple sequences of modulated transmit symbols of duration T_I . The sequences are transmitted simultaneously on N equidistant orthogonal carrier frequencies f_n , $n = 0, \dots, N-1$, as shown in Fig. 1. Orthogonal subcarriers are obtained by applying a carrier spacing of $\Delta f_I = 1/T_I$, so the baseband carrier frequencies are $f_n = n/T_I$. A single OFDM symbol is the summation of N parallel symbols of the orthogonal subcarriers

$$s_{I,\text{sym}}[k] = \sum_{n=0}^{N-1} d_{Tx}[n] e^{j2\pi \frac{kn}{N}}. \quad (4)$$

An OFDM block consists of M subsequent OFDM symbols. The complex OFDM signal model with carrier frequency f_c yields

$$s_I(t) = \sum_{m=0}^{M-1} \sum_{n=0}^{N-1} d_{Tx}(m, n) e^{j2\pi(f_n + f_c)t} \text{rect}\left(\frac{t - mT_I}{T_I}\right). \quad (5)$$

III. INTERFERENCE BY OFDM RADARS

In this section, the interference signal and power level at the receiver that influence the result of the radar evaluation are derived. The interfering power at the chirp sequence radar receiver can be illustrated graphically in a frequency versus time diagram of both signals as shown in Fig. 2. At every point in time, the OFDM transmit power is spread over the bandwidth B_I that is much larger than the receiver bandwidth B_{Rx} of the chirp sequence radar. It is assumed that the interference level is proportional to the intersection area (gray) given by $2 B_{Rx} T_c$.

The interfering OFDM signal transmitted at distance R_I and received at the chirp sequence radar is (5) delayed by $\Delta t_I = R_I/c$. The complex representation of the interfering signal yields

$$y_I(t) = A s_I(t - \Delta t_I) \quad (6)$$

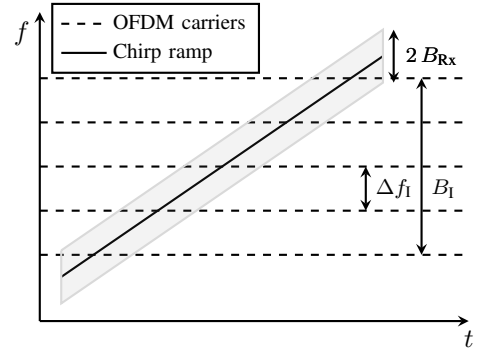


Fig. 2. Interference of a single chirp ramp (—) by multiple OFDM carriers (---) with carrier spacing Δf_I . The OFDM bandwidth is B_I . Interference is caused by OFDM carriers as long as they are located within the receiver bandwidth B_{Rx} . The received interference power is proportional to the gray shaded area given by $2 B_{Rx} T_c$.

with the signal amplitude A . The interfering signal (6) is mixed with the chirp signal (1). Since the interference is additive, the disturbed baseband signal yields

$$\tilde{s}_{IF}(t) = s_{IF}(t) + y_I(t) s_{Tx}(t). \quad (7)$$

The signal is filtered by a lowpass filter with bandwidth B_{Rx} and evaluated by a two-dimensional Fourier transform.

To evaluate the effect of the OFDM interference signal, the expected power levels in the resulting range-Doppler spectrum are derived in the following.

A. Noise Power Level

The noise power in a receiver with noise figure F and receiver bandwidth B_{Rx} is

$$P_{\text{noise}} = k T 2 B_{Rx} F, \quad (8)$$

with the Boltzmann constant k and temperature $T = 300$ K.

B. Target Reflection Power

The power received from a target at distance R is described by the radar equation:

$$P_{Rx} = \frac{P_{Tx} G_{Tx} G_{Rx} \lambda^2 \sigma}{(4\pi)^3 R^{3.5}}. \quad (9)$$

The distance R and the RCS σ are target dependent values. P_{Tx} , G_{Tx} , and G_{Rx} are the radar transmit power, and transmit and receive antenna gains, respectively. The exponent 3.5 is used instead of 4 since it yields better results in automotive scenarios according to our experience from many measurements. In the range-Doppler spectrum, the target power level is increased by the integration gain $G_{\text{integ}} = L N_{\text{Samples}}$, with N_{Samples} the number of samples in a single frequency ramp, and L the number of ramps.

C. Interference Power Level

The interference power of the OFDM interferer is derived based on the assumption that an OFDM signal is composed of

multiple CW signals. The power level of an interfering CW or FMCW radar at a distance of R_I is described using [1] by

$$P_{R_x,CW} = \frac{P_{T_x,I} G_{T_x,I} G_{R_x} \lambda_I^2}{(4\pi R_I)^2}. \quad (10)$$

$P_{T_x,I}$ and $G_{T_x,I}$ are the transmit power and transmit antenna gain of the interfering radar, and G_{R_x} is the antenna gain of the interfered radar in (9). Using equation (17) of [4], the maximum power of an interfering CW radar in the range-Doppler spectrum yields

$$|S_I(f)|^2 \propto \frac{P_{R_x,CW}}{\mu N_{FFT}} \quad (11)$$

with

$$\frac{1}{\mu} = T_I f_s = \frac{2B_{R_x}}{B/T_c} f_s. \quad (12)$$

The factor $1/\mu$ describes the number of samples affected by interference, given by the interference duration T_I (cf. [3]) and the sampling rate f_s . N_{FFT} is the number of evaluated Fourier coefficients. The equation shows that the interference power increases linearly with the number of samples affected by interference.

The interfering OFDM signal can be seen as an accumulation of N_I CW signals with different frequencies. Because of the multiple OFDM modulation symbols, those interference contributions are added up non-coherently in the range-Doppler spectrum. If $N_I \leq N$ of the subcarriers are located within the bandwidth B occupied by the chirp sequence radar, the overall interference power increases proportional to N_I :

$$P_I = \frac{N_I}{\mu N_{FFT}} P_{R_x,CW}. \quad (13)$$

Note that the change in wavelength between the different OFDM subcarriers is neglected here.

IV. SIMULATION AND RESULTS

A simple traffic scenario with two vehicles is assumed for the simulation and evaluation. One vehicle is equipped with the chirp sequence radar, the second vehicle with the interfering OFDM radar. To analyze the effect of different signal parameters on the interference, different radar configurations are used for the simulation.

An overview of the assumed radar parameters of the chirp sequence and the OFDM radar are shown in Table I. For the chirp radar transmitter a transmit antenna gain of 24 dBi and a transmit output power of 3 dBm is assumed. For the receiver, an antenna gain of 14 dBi, a receive bandwidth of $B_{R_x} =$

TABLE I
RADAR PARAMETERS OF THE CHIRP SEQUENCE AND OFDM RADAR

Paramter	Symbol	Chirp sequence	OFDM
Transmit power	P_{T_x}	3 dBm	0 dBm
Transmit gain	G_{T_x}	24 dBi	25 dBi
Receive gain	G_{R_x}	14 dBi	—

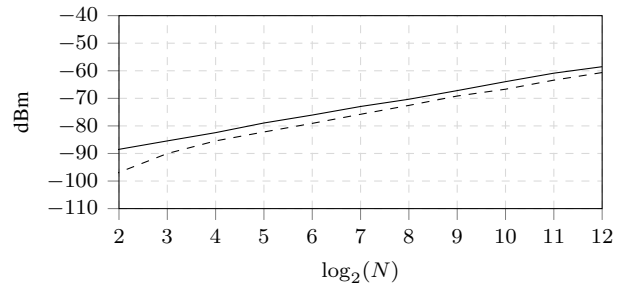


Fig. 3. Mean interference level in dBm for different carrier densities for a chirp bandwidth of $B = 400$ MHz (—) and $B = 2$ GHz (---)

5 MHz and a noise figure of $F = 6$ dB are selected. This results in a noise power level of $P_{noise} = -97.8$ dBm, see (8).

For the target vehicle, that is also the interferer, an RCS of $\sigma = 10 \text{ m}^2$, a distance of $R = R_I = 10$ m and a relative velocity of $v = 10$ m/s is assumed. According to (9), this leads to $P_{R_x} = -65$ dBm. Another 6 dB loss for both the mixing process in the simulation and the use of a cosine chirp signal instead of a complex signal must be taken into account. With an integration gain of the Fourier transforms (including a Hann-window) of 35 dB, a power level of

$$P_{target} = P_{R_x} - 6 \text{ dB} - 6 \text{ dB} + G_{integ} = -42 \text{ dBm} \quad (14)$$

is achieved. The dotted line in Fig. 4 is the resulting spectrum in range direction in case of no interference. It can be seen that the assumed values for the target peak and noise floor are reflected in the simulations.

The OFDM radar is simulated with a transmit antenna gain of 25 dBi and a transmit power of 0 dBm (see Table I). This results in an interference power level (10) of $P_{R_x,CW} = -51$ dBm. Including a loss of 6 dB in the mixing process, the interference level in the range-Doppler spectrum is -95 dBm and -100 dBm according to (11) for a chirp bandwidth of 400 MHz and 2 GHz, respectively.

In simulations, the influence of carrier density, bandwidth and modulation order of the OFDM interferer were analyzed. First, a fixed OFDM bandwidth of $B_I = 1.16$ GHz and $N = 4, 8, 16, \dots, 4096$ equidistant subcarriers were simulated. A doubling of the number of subcarriers halves the subcarrier spacing. It is expected that for both chirp sequence configurations the doubling of the number of carriers equals an increase of 3 dB of the interference floor. Fig. 3 shows the mean interference level for different number of subcarriers verifying this assumption.

In Fig. 4 the cut through the radar spectrum at $v = 10$ m/s is plotted for the 400 MHz and 2 GHz chirp radar. The curves for no interference, 128 subcarriers, and 4096 subcarriers are plotted. For 4096 carrier, the resulting SNR is only about 15 dB. In this case, targets with a low RCS or with a larger distance to the radar are very likely covered by the interference and may not be detected.

We further investigated the influence of different OFDM bandwidths with a fixed carrier spacing of $\Delta f = 1.14$ MHz.

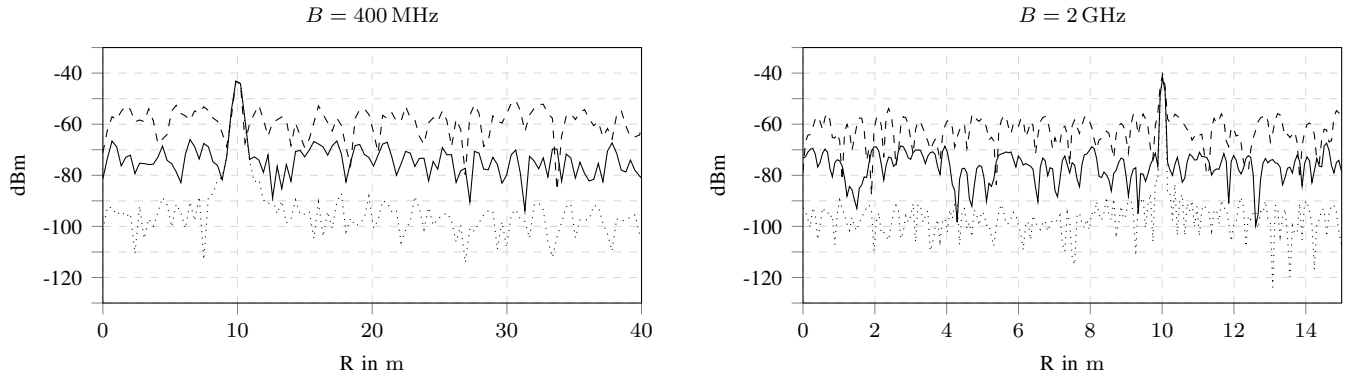


Fig. 4. Range profile simulation results of a target at 10 m using a chirp sequence bandwidth of 400 MHz and 2 GHz. Results are shown for the cases of no interference (.....), 128 (—), and 4096 (---) interfering OFDM subcarriers.

This is done by stepwise increasing the number of equidistant OFDM subcarriers. In Table II, the number of OFDM subcarriers, the corresponding OFDM bandwidths B_I , and the resulting interference-induced mean noise floors of the simulations are listed. The points at which the OFDM bandwidth exceeds the chirp bandwidth where no further increase of the noise level is expectable and observable are highlighted in bold. The limit noise level for both chirp configurations is the same. This can be explained by Fig. 2. The mean interference power in the range-Doppler spectrum depends on the subcarrier density and the value of the gray area which equals $2B_{RX}T_c$. For both chirp sequence configurations all these parameters are the same. In the table, it can also be observed that if the interference bandwidth doubles, there is no linear increase of 3 dB in the noise floor. This is because the window function applied in signal processing takes a different influence on the power of each interfering subcarrier, depending on the carrier's frequency. This is a similar effect as it was reported for CW radar interference in [4].

For the modulation order analysis, PSK modulations of $k=2, 4, 8, 16$ are analyzed. No significant differences or trends can be identified by the simulations.

V. CONCLUSION

In this paper, the interference effects of a wideband automotive OFDM radar on a chirp sequence radar are investigated. The expected noise and interference power levels are derived. The influence of OFDM subcarrier spacing, bandwidth, and modulation order are analyzed by simulations. The modulation order for PSK has no influence on the interference level.

TABLE II
INTERFERENCE POWER LEVEL P_I FOR AN OFDM CARRIER SPACING OF $\Delta f = 1.14$ MHz FOR DIFFERENT INTERFERENCE BANDWIDTHS

N	128	256	512	1024	2048
$B_I = N \Delta f_I$ in MHz	146	292	584	1167	2335
P_I in dBm ($B=400$ MHz)	-73	-65	-64	-64	-64
P_I in dBm ($B=2$ GHz)	-104	-90	-77	-67	-64

An increase of OFDM subcarriers within the chirp sequence bandwidth increases the mean noise floor significantly, so that small targets may be covered by the increased noise floor. An increase of the chirp bandwidth has no effect on the interference level as long as the chirp bandwidth does not exceed the OFDM bandwidth.

ACKNOWLEDGMENT

The research leading to these results was conducted within the Tech Center a-drive. Responsibility for the information and views set out in this publication lies entirely with the authors.

REFERENCES

- [1] G. M. Brooker, "Mutual Interference of Millimeter-Wave Radar Systems," *IEEE Transactions on Electromagnetic Compatibility*, vol. 49, no. 1, pp. 170–181, Feb. 2007.
- [2] M. Goppelt, H.-L. Blöcher, and W. Menzel, "Automotive radar - investigation of mutual interference mechanisms," *Advances in Radio Science*, vol. 8, pp. 55–60, 2010. [Online]. Available: <http://www.adv-radio-sci.net/8/55/2010/>
- [3] D. Oprisan and H. Rohling, "Analysis of Mutual Interference between Automotive Radar Systems," in *International Radar Symposium (IRS)*, 2005.
- [4] T. Schipper, M. Harter, T. Mahler, O. Kern, and T. Zwick, "Discussion of the operating range of frequency modulated radars in the presence of interference," *International Journal of Microwave and Wireless Technologies*, vol. 6, pp. 371–378, 2014.
- [5] M. Barjenbruch, D. Kellner, K. Dietmayer, J. Klappstein, and J. Dickmann, "A Method for Interference Cancellation in Automotive Radar," in *IEEE MTT-S International Conference on Microwaves for Intelligent Mobility (ICMIM)*, Apr. 2015, pp. 1–4.
- [6] C. Fischer, M. Goppelt, H.-L. Blöcher, and J. Dickmann, "Minimizing interference in automotive radar using digital beamforming," *Advances in Radio Science*, vol. 9, pp. 45–48, 2011. [Online]. Available: <http://www.adv-radio-sci.net/9/45/2011/>
- [7] J. Bechter, K. Eid, F. Roos, and C. Waldschmidt, "Digital Beamforming to Mitigate Automotive Radar Interference," in *IEEE MTT-S International Conference on Microwaves for Intelligent Mobility (ICMIM)*, May 2016, pp. 1–4.
- [8] J. Bechter, C. Sippel, and C. Waldschmidt, "Bats-Inspired Frequency Hopping for Mitigation of Interference Between Automotive Radars," in *2016 IEEE MTT-S International Conference on Microwaves for Intelligent Mobility (ICMIM)*, May 2016, pp. 1–4.
- [9] N. Levanon, "Multifrequency complementary phase-coded radar signal," *IEE Proceedings - Radar, Sonar and Navigation*, vol. 147, no. 6, pp. 276–284, 2000.
- [10] V. Winkler, "Range Doppler Detection for Automotive FMCW Radars," in *Proceedings of the 14th European Radar Conference*, Oct. 2007, pp. 166–169.